Catalysis Today 176 (2011) 126–130

Contents lists available at ScienceDirect

Catalysis Today

journal homepage: www.elsevier.com/locate/cattod

Catalytic decomposition of nitrogen oxides from coal combustion flue gases on $CeZrO_2$ supported Cu catalysts

Agata Łamacz*, Andrzej Krztoń, Gérald Djéga-Mariadassou

Polish Academy of Sciences, Centre of Polymer and Carbon Materials, Marii Curie-Sklodowskiej 34, 41-819 Zabrze, Poland

ARTICLE INFO

Article history:
Received 5 November 2010
Received in revised form
23 December 2010
Accepted 24 January 2011
Available online 11 February 2011

Keywords:
deNO$_x$
Toluene
Ceria–zirconia
Copper

ABSTRACT

The paper deals with ceria–zirconia supported copper catalysts in NO reduction by toluene. Catalysts were characterized by XRD and H_2-TPR. The deNO$_x$ temperature window was estimated by NO-TPD experiments which revealed two NO desorption areas. The activity and temperature range for deNO$_x$ reaction were being observed during temperature programmed deNO$_x$ reaction (TPSR) in the presence of toluene. NO$_x$ decomposition, starting above 200 °C, was accompanied by total oxidation of toluene. Catalytic tests performed in stationary conditions revealed that the most active in C_7H_8-SCR of NO$_x$ is Cu(4)/CeZrO$_2$.

1. Introduction

The combustion of still very popular fossil fuels in utility and in industrial boilers leads to the release of CO, volatile organic compounds (VOCs), polycyclic aromatic hydrocarbons (PAHs) and nitrogen oxides (NO$_x$). The amounts of these pollutants depend on the type of coal and the excess of oxygen used in combustion process [1]. For instance, application of approximately 4% of oxygen, at the temperatures above 800 °C, leads to 110 ppm of NO$_x$ and mg/Nm^3 of both VOCs (mainly aromatic hydrocarbons) and PAHs. The VOCs released during coal combustion consists mainly of benzene, toluene and xylenes [1–3] where the two first are the most numerous. In order to preserve the global environment, efficient deNO$_x$ technologies have been developed. Ceria–zirconia based catalytic systems are found to be very good in selective catalytic reduction of NO$_x$ by hydrocarbons and attracted much attention because of their high oxygen storage capacity (OSC). The disadvantage of pure CeO_2 is its poor thermal stability. The addition of ZrO_2 strongly improves ceria OSC, redox properties, thermal resistance and catalytic activity at lower temperatures [4,5].

The aim of this work was to find active catalyst for NO$_x$ reduction from coal combustion using toluene as a reducing agent. The use of such "internal" reductor facilitates decomposition of two kinds of noxious products of coal combustion: NO$_x$ and VOCs. Some studies of C_7H_8-SCR of NO$_x$ on Cu-ZSM-5 and Au/Al_2O_3 revealed, that toluene presence in the gas phase has negative effect on catalysts activity in deNO$_x$ process [6,7]. In the case of ceria–zirconia supported catalyst, the adsorption of aromatics (like toluene) is more favorable to deNO$_x$ process than of light hydrocarbons [8]. This is the advantage of ceria–zirconia supported catalysts over zeolites and alumina catalysts for the sake of their application in reduction of NO$_x$ that are present in the flue gases from coal combustion. Due to the high price of rhodium, that was found to be a good catalyst in deNO$_x$ reaction [9], we concentrated in our studies on cheaper metals like copper, supported on $Ce_{0.63}Zr_{0.37}O_2$, which was selected as the most active among three studied by Adamowska et al. [10] $Ce_xZr_{1-x}O_2$ ($x = 0.17, 0.62, 0.8$) solid solutions.

2. Experimental

The commercial ceria–zirconia $Ce_{0.63}Zr_{0.37}O_2$ solid solution (named "CZ" hereafter), obtained via hydrothermal synthesis from nitrate precursors, was provided by Rhodia Company. Catalysts were prepared by incipient wetness impregnation of formerly calcined at 500 °C for 5 h CZ with aqueous solutions of copper nitrate. After impregnation and drying at 110 °C, catalysts were calcined at 550 °C for 2 h. Thereby, three catalysts containing nominally 2, 4 and 10 wt% of copper were obtained.

Specific surface area (SSA) measurements were performed using Sorptomatic 1800 Carlo Erba Instrument equipped in MILESTON100 software. The samples were pretreated in vacuum at 250 °C for 12 h before experiments. Surface areas were determined by physical adsorption of N_2 at the temperature of liquid nitrogen, using BET equation.

---

* Corresponding author. Tel.: +48 032 2716077; fax: +48 032 2382831.
E-mail address: agata.lamacz@cmpw-pan.edu.pl (A. Łamacz).

0920-5861/$ – see front matter © 2011 Elsevier B.V. All rights reserved.
doi:10.1016/j.cattod.2011.01.032

Table 1
Composition by weight and specific surface area of ceria–zirconia and copper catalysts.

Catalyst	Composition (wt%)				SSA (m^2/g)
	Ce	Zr	O	Cu	
CZ	52.6	21.45	25.95	–	136
Cu(2)/CZ	51.67	20.85	25.53	1.95	115
Cu(4)/CZ	49.5	20.62	26.15	3.73	107
Cu(10)/CZ	45.76	19.67	26.26	8.31	99

XRD patterns were acquired using Siemens 500D diffractometer employing Cu-Kα radiation (λ = 1.54 Å). Crystallographic structures of the samples and Miller indices (h k l) of diffraction line were established by comparing with bibliographic data (JCPDS published by Joint Committee on Powder Diffraction Standards).

Hydrogen-temperature programmed reduction (H_2-TPR) measurements were carried out in a flowing gas mixture containing 5 vol.% of H_2 in Ar. The temperature was increased linearly up to 1000 °C, with a heating rate of 7.5 °C/min and a total flow rate of 30 mL/min.

Temperature programmed desorption (TPD) of NO was performed in a U-type reactor. The outlet gas was analyzed using NO, NO_2, NO_x, CO_2 and FID specific detectors. Before NO-TPD, catalyst sample was treated by gas mixture consisted of NO (250 ppm), O_2 (5 vol.%) and Ar as complement, at room temperature (RT) for 90 min. After NO adsorption at RT, sample was purged by Ar for 1 h. TPD was carried out in O_2 (5 vol.% in Ar), with a flow-rate of 250 mL/min and a heating rate of 3 °C/min from RT to 550 °C.

TPSR experiments and steady state experiments were carried out in the gas mixture of NO (250 ppm), C_7H_8 (250 ppm), O_2 (5 vol.%) and Ar as complement, under atmospheric pressure, with a total flow-rate of 250 mL/min and a GHSV = 10000 h^{-1}. During TPSR experiments, temperature was increased linearly by 3 °C/min from RT to 500 °C. The composition of the outlet gas during isothermal experiments was analyzed until NO, NO_2 and CO_2 concentrations were stable. During steady state experiments, the temperature was decreased from 500 to 200 °C by 100 °C.

Before each TPR, TPD and TPSR catalysts were calcined in situ at 500 °C for 2 h in 5 vol.% of O_2 in Ar.

3. Results and discussion

Chemical constitution and specific surface areas (SSA) of ceria–zirconia support and copper catalysts are presented in Table 1. It is observed, that with increasing metal loading specific surface area decreases. However, $CeZrO_2$ reveals very high SSA, even after doping with copper.

3.1. X-ray diffraction

XRD method was used for the identification of support and metals crystallographic phases. XRD pattern of ceria–zirconia, as a reference to XRD patterns of copper catalysts is presented in Fig. 1a. The diffraction peaks of CZ are symmetrical, what speaks for the formation of single ceria–zirconia solid solution. $Ce_{0.62}Zr_{0.38}O_2$ reveals regular crystallographic structure [11,12]. XRD patterns of copper catalysts are shown in Fig. 1(b–d). No typical for monoclinic CuO crystalline reflex are observed on Cu(2)/CZ and Cu(4)/CZ XRD patters. In the case of low loaded Cu/CZ, copper species are probably highly dispersed on the support surface. All lattice vacancies are accessible for Cu^{2+}, thus metal-support interaction is favored and high metal phase dispersion may occur. It was reported by Liu [13] that ceria-rich support disperse copper species more effectively than zirconia-rich one. Besides, no shifts of ceria–zirconia reflex are noticed on XRD patterns of Cu/CZ, therefore it can be assumed that copper does not insert into bulk lattice to form $CuCeZrO_x$ solid solution. Diffraction peaks of CuO crystalline are visible only on XRD pattern of Cu(10)/CZ (Fig. 1d). High Cu loading takes effect in Cu^{2+} agglomeration which is probably caused by metal–metal interaction. Impregnation of CZ by copper results in the increase of grain size, nevertheless it does not influence on the lattice parameters of $CeZrO_2$. Main diffraction peaks of CuO are observed at $2\theta = 35.6°$, 38.8°, 63.8° and 68.4°, whereas two later are hardly recognizable.

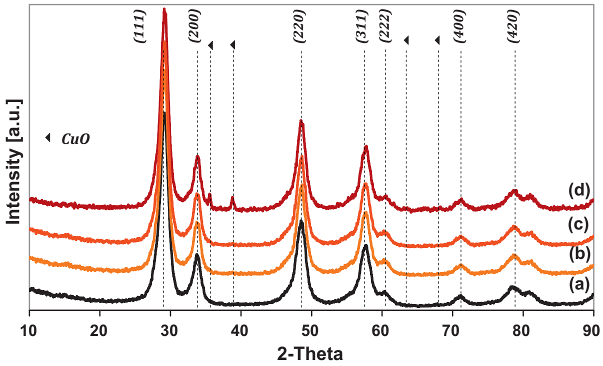

Fig. 1. XRD patterns for CZ (a), Cu(2)/CZ (b), Cu(4)/CZ (c) and Cu(10)/CZ (d).

3.2. Temperature programmed reduction

Profiles of H_2-TPR for ceria–zirconia support and copper catalysts are illustrated in Fig. 2. Temperature of CZ reduction differs from the temperature of hydrogen consumption by metal based catalysts. It has been discovered that CeO_2 is reduced at two temperature regions: at 500 °C – reduction of surface capping oxygen and above 800 °C – bulk reduction. The addition of ZrO_2 increases superficial reducibility of ceria and shifts its reduction into lower temperatures. Nevertheless, the reduction of Zr^{4+} occurs above 1000 °C [14,15] thus, H_2-TPR profiles of CZ and further presented Cu(*x*)/CZ do not contain reduction of zirconium. Ceria reduction, observed at 500 °C, leads to formation of oxygen vacancies (V_o) that can enhance ionic conductivity in CeO_2 and fulfil an important role in catalysis:

$$2Ce^{4+} + O^{2-} + H_2 \rightarrow 2Ce^{3+} + H_2O + V_o$$

Substitution of Ce^{4+} by smaller Zr^{4+} ions leads to stress in the lattice what facilitates oxygen extraction from CeO_2. Introduction of zirconium to CeO_2 lattice improves oxygen mobility due to structure change: from regular to tetragonal [16]. However, too high concentration of ZrO_2 results in decrease of oxygen mobility and

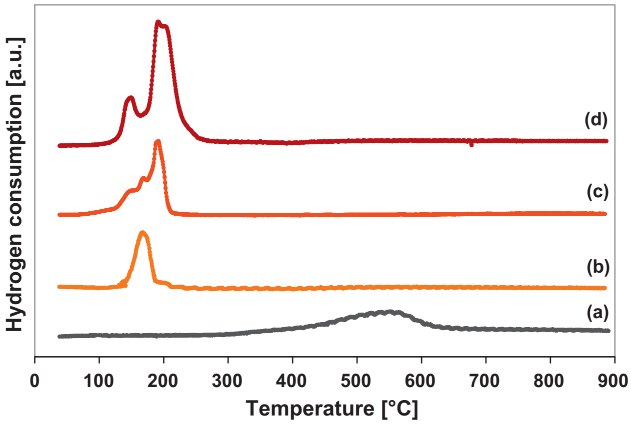

Fig. 2. H_2-TPR profiles for CZ (a), Cu(2)/CZ (b), Cu(4)/CZ (c) and Cu(10)/CZ (d).

furthermore, it has negative effect on reduction of CeO_2 in its internal layer [17]. H_2-TPR profile for CZ is presented in Fig. 2a. Shoulder at 350 °C refers to surface reduction or nano-particle CeO_2. It has been reported, that in case of nano-particle ceria, desorption of O_2 may occur even at 350 °C [18] what can be explained by the interstitial character of such O_2. It has been presented that in comparison to lattice O_2, interstitial oxygen is much easier to remove [19] or in other words, surface diffusion of oxygen is much faster than in the bulk [20] and furthermore, it depends of the temperature and concentration of oxygen vacancies [21]. The reduction peak at 550 °C on TPR profile for CZ is assigned to reduction of bulk CeO_2 ($Ce^{4+} \rightarrow Ce^{3+}$) [22]. H_2-TPR profile of copper catalysts revealed that impregnation of ceria–zirconia even by small amount of Cu drastically decreases the temperature of its reduction. At low temperature range at least two reduction peaks are observed. These peaks are contributed to concurrent reduction of different types of copper species and surface oxygen from ceria–zirconia. The maximum of hydrogen consumption for Cu(2)/CZ (Fig. 2b) occurring at 165 °C is assigned to reduction of highly dispersed CuO species and/or isolated Cu^{2+} ions, that are strongly interacting with $CeZrO_2$. During impregnation process, vacancies of ceria–zirconia are accessible for copper ions, therefore metal phase, strongly interacting with the support is well dispersed [13,23]. In the case of Cu(4)/CZ (Fig. 2c) two small reduction peaks are visible: at 150 and 170 °C. These peaks are contributed to the reduction of isolated Cu^{2+} ions and well dispersed CuO species whereas hydrogen consumption at 190 °C is assigned to reduction of bulk-like CuO. Peaks observed at 150 and 170 °C overlap in the case of Cu(10)/CZ and one reduction peak, coming from highly dispersed CuO species is observed. The higher the dispersion is, the lower the temperature of reduction of CuO species. Reduction of bulk-like CuO is noticed at 200 °C, whereas its intensity increases with metal loading. It has been found that the higher Cu loading, the lower temperature of bulk-like CuO reduction [24]. Introduction of copper greatly enhances red-ox properties of ceria, probably due to oxygen transfer. Good electrophilic properties of metastable CuO have positive effect on its oxygen transfer capacity, so even at high reductive atmosphere, an equilibrium between ceria and copper cations can stabilize cationic copper species [25–27]:

$$Ce^{4+} + Cu^{+} \leftrightarrow Ce^{3+} + Cu^{2+}$$

Therefore, oxygen transfer is not limited to ceria lattice but it also includes migration between ceria and supported metal [28]. Moreover, the rate of oxygen diffusion is determined by temperature and concentration of oxygen vacancies.

Temperature programmed desorption of NO (TPD) on CZ and Cu(10)/CZ are shown in Fig. 3. It is observed that due to high specific surface area of CZ, 90 min adsorption at room temperature was not sufficient for ceria–zirconia saturation with NO (Fig. 3a). Temperature increase resulted in two desorption areas:

1) low temperature desorption of NO
2) high temperature desorption of NO_x, that is a sum of NO and NO_2

The presence of nitrogen dioxide in the gas phase at higher temperatures is caused by oxidation of NO. Nevertheless, for the sake of thermodynamic limitations, NO_2 disappears with further increase of temperature:

$$NO_2 = NO + O_2$$

Such TPD profile is typical for all copper catalysts (TPDs of Cu(2)/CZ and Cu(4)/CZ are not shown here). In the case of CZ, low temperature desorption is extended from 40 to 200 °C. Desorption of NO_2 is observed from 290 to 360 °C. Afterwards, NO_2 is being decomposed to NO. The maximum of NO_x desorption is noticed at 450 °C. NO-TPD profile for Cu(10)/CZ is shown in Fig. 3b. The first, interesting phenomenon that distinguishes this catalysts from CZ is great adsorption of NO. Desorption peaks of NO_x are also more intensive and occur at lower temperatures (140 and 350 °C) than in the case of CZ and not presented here Cu(2)/CZ and Cu(4)/CZ. Low temperature NO_2 desorption on CZ and Cu(x)/CZ begins around 90 °C and is the most important in the case of Cu(10)/CZ. From 350 °C, NO_2 commences to be decomposed to NO. Thus, an assumption that NO activation on ceria–zirconia supported catalysts increases with Cu loading can be made. Adsorption of NO per 1 g of catalysts is shown in Table 2. It was calculated that NO adsorption increases with metal loading, however the difference between Cu(4)/CZ and Cu(10)/CZ is insignificant. Well dispersion of copper species in the case if Cu(4)/CZ provides more active sites for NO adsorption than in the case of high loaded Cu/CZ, where CuO is present in bulk-like form.

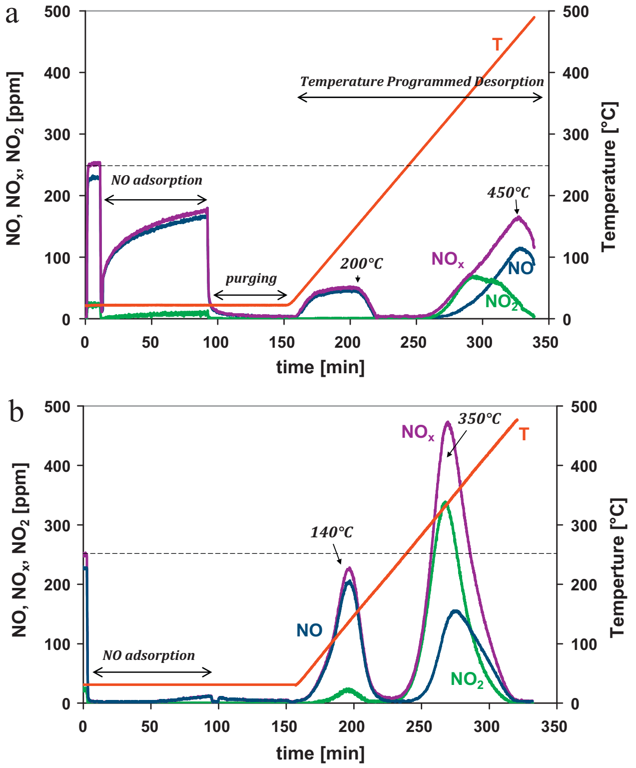

Fig. 3. Temperature programmed desorption of NO on CZ (a) and Cu(10)/CZ.

3.3. Temperature programmed surface reaction

Catalytic tests of deNO_x reaction in temperature programmed conditions were performed in order to determine the temperature window for NO_x decomposition to N_2. In general, ceria–zirconia support as well as copper catalysts had similar shape of TPSR plots, however the temperature and percentage of NO_x conversion vary for particular catalysts. In this paper only TPSR results on repre-

Table 2
NO adsorption per 1 g of catalyst at RT.

Catalyst	NO adsorption (μmol/g)
CZ	82
Cu(2)/CZ	101
Cu(4)/CZ	**142**
Cu(10)/CZ	**148**

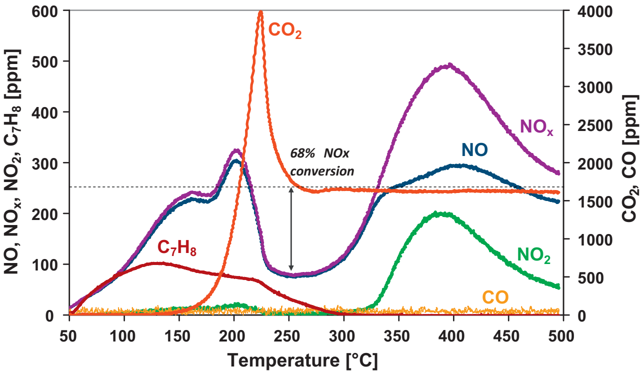

Fig. 4. TPSR on Cu(4)/CZ (250 ppm NO, 250 ppm C_7H_8, 5 vol.% O_2, Ar).

sentative, Cu(4)/CZ are reported (Fig. 4). Total oxidation of toluene starts at 140 °C, while NO_x and NO_2 desorption occur from 175 °C. A considerable increase of CO_2 concentration is also observed from 175 °C (with maximum at 225 °C). Nevertheless, the decrease of C_7H_8 concentration does not correspond to CO_2 formation, which is much bigger that it would arise from C_7H_8 loss. Such intensive CO_2 production comes from activation of toluene (HC) by NO_2. Formed on the surface nitro-organic compounds are unstable and decompose to oxygenates ($C_xH_yO_z$), which are subsequently reacting with NO to nitrogen, CO_2 and H_2O. Therefore, NO desorption around 200 °C is caused by decomposition of RNO_x to oxygenates. Rapid CO_2 production at this temperature with accompanying decrease of NO concentration arises from the reaction of $C_xH_yO_z$ with NO what results in N_2 production (96% selectivity in the case of TPSR on Cu(4)/CZ at 250 °C). Thus, NO_x decomposition to N_2 is possible from 215 to 325 °C. The maximal NO_x conversion (68%) is noticed around 250 °C. For comparison, not presented here CZ revealed 35% of NO_x conversion at 320 °C while Cu(2)/CZ and Cu(10)/CZ exhibited conversions of 50% (at 275°) and 58% (at 270 °C), respectively. After sudden combustion of cumulated toluene, its conversion to CO_2 on Cu(4)/CZ levels at 96%. From 330 °C, some part of NO is oxidized to NO_2. N_2O was not formed during temperature C_7H_8-SCR of NO reaction on CZ and Cu(x)/CZ. Performed tests revealed that impregnation of ceria–zirconia by 4 wt% of copper decrease the temperature of deNO_x to 250 °C reaction and increased NO_x and toluene conversions.

3.4. *Catalytic runs in stationary conditions*

Results of catalytic tests for deNO_x reaction carried out with an excess of O_2, in stationary conditions for all synthesized catalysts, and conversions of toluene to CO_2 are given in Table 3. It appears, as previously explained, that the most active catalyst is Cu(4)/CZ with only 30% of NO_x conversion. GC analysis revealed 63% selectivity to N_2 at 270 °C. It is also observed, that the addition of copper influences the temperature of maximal NO_x conversion, shifting it into lower values.

Table 3
Results of catalytic tests in stationary conditions. T_{max} is the temperature of maximal NO_x conversion.

Catalyst	T_{max} of deNO_x (°C)	NO_x conversion (%)	C_7H_8 conversion to CO_2 (%)
$CeZrO_2$	295	12	46
Cu(2)/CZ	260	17	33
Cu(4)/CZ	**255**	**30**	**71**
Cu(10)/CZ	250	20	63

4. Conclusions

H_2-TPR characteristics for copper catalysts revealed that there are two CuO species on Cu(4)/CZ and Cu(10)/CZ: well dispersed CuO species and bulk-like CuO, non-associated with ceria–zirconia. Low temperature reduction of Cu/CZ indicates high oxygen mobility on the surface and within the bulk. Relatively free movement of oxygen for ceria to copper species arises from the interaction between Cu and CeO_2.

Presented data shown that nano-particle $Ce_{0.62}Zr_{0.38}O_2$ reveal good activity in SCR of NO, however the highest NO_x conversions to N_2 was demonstrated by Cu(4)/CZ. Nevertheless, these catalysts are still less active in than rhodium ones. Selected ceria–zirconia support, of specified Ce/Zr molar ratio, is characterized by the most significant formation of oxygen vacancies. The activity of copper catalysts in deNO_x reaction was first uprating with Cu content - a great increase of NO_x conversion was observed after the increase of Cu loading from 2 to 4 wt%. Subsequent raising of metal loading to 10 wt% resulted in activity decrease – Cu(10)/CZ was less active than Cu(4)/CZ. The loading of 4 wt% appeared to be the optimal. This catalyst revealed good dispersion of CuO on CZ surface what was confirmed by XRD and H_2-TPR analysis. Cu(4)/CZ exhibited the highest NO_x conversion during catalytic tests carried in the modes of TPSR and in stationary conditions.

Acknowledgements

Authors acknowledge financial support of the International Group of Research (GDRI) “Catalysis for Environment: Depollution, Renewable Energy and Clean Fuels” and Prof. Patrick Da Costa for scientific support.

References

[1] H.K. Chagger, J.M. Jones, M. Pourkashanian, A. Williams, A. Owen, G. Fynes, Fuel 78 (1999) 1527–1538.
[2] J.D.N. Pone, K.A.A. Hein, G.B. Stracher, H.J. Annegarn, R.B. Finkleman, D.R. Blake, J.K. McCormack, P. Schroeder, Int. J. Coal Geol. 72 (2007) 124–140.
[3] G. Fernandez-Martinez, P. Lopez-Mahia, S. Muniategui-Lorenzo, D. Prada-Rodriguez, E. Fernandez-Fernandez, Atmos. Environ. 35 (2001) 5823–5831.
[4] A.B. Ross, J.M. Jones, S. Chaiklangmuang, M. Pourkashanian, A. Williams, K. Kubica, J. Andersson, Fuel 81 (2002) 571–582.
[5] L.F. de Mello, M. Baldanza, F.B. Noronha, M. Schmal, Catal. Today 85 (2003) 3–12.
[6] K. Arve, F. Klingstedt, K. Eränen, L.-E. Lindfors, D.Y. Murzin, Catal. Lett. 105 (2005) 133–136.
[7] J.P. Breen, R. Burch, C. Hardacre, C.J. Hill, B. Krutzsch, B. Bandl-Konrad, E. Jobson, L. Cider, P.G. Blakeman, L.J. Peace, M.V. Twigg, M. Preis, M. Gottschling, Appl. Catal. B: Environ. 70 (2007) 36.
[8] M. Adamowska, S. Muller, P. Da Costa, A. Krzton, P. Burg, Appl. Catal. B: Environ. 74 (2007) 278–289.
[9] M. Adamowska, A. Krztoń, M. Najbar, J. Camra, G. Djega-Mariadassou, P.Da. Costa, Appl. Catal. B: Environ. 90 (2009) 353–544.
[10] M. Adamowska, A. Krzton, M. Najbar, P. Da Costa, G. Djega-Mariadassou, Catal. Today 137 (2008) 288–291.
[11] P. Fornasiero, R. Di Monte, G. Rao Ranga, J. Kaspar, S. Mmerani, A. Trovarelli, M. Graziani, J. Catal. 151 (1995) 168.
[12] D. Terrible, A. Trovarelli, J. Llocra, C. De Leitenburg, C. Dolcetti, Catal. Today 43 (1998) 79.
[13] W. Liu, M. Flytzani-Stephanopoulos, Catal. Today 28 (1996) 391.
[14] E. Diaz, B. de Rias, R. Lopez-Fonsees, S. Ordonez, J. Chromatogr. A 1116 (2006) 230.
[15] R. Di Monte, J. Kaspar, Catal. Today 100 (2005) 27.
[16] G. Vlaic, R. Di Monte, P. Fornasiero, E. Fonda, J. Kaspar, M. Graziani, J. Catal. 182 (1999) 378–389.
[17] R. Di Monte, P. Fornasiero, M. Graziani, J. Kaspar, J. Alloys Compd. 877 (1998) 275–277.
[18] S. Kim, R. Merkle, J. Maier, Surf. Sci. 549 (2004) 196.
[19] E. Mamontov, T. Egami, R. Brezy, M. Koranne, S. Tyagi, J. Phys. Chem. B 104 (2000) 11110.
[20] D. Martin, D. Duprez, J. Phys. Chem. 100 (1996) 9429–9438.

[21] J.W. Park, J.H. Jeong, W.L. Yoon, H. Jung, H.T. Lee, D.K. Lee, Y.K. Park, Y.W. Rhee, Appl. Catal. A: Gen. 274 (2004) 25–32.
[22] E. Aneggi, M. Boaro, C. De Leitenburg, G. Dolcetti, A. Trovarelli, J. Alloys Compd. 408–412 (1996) 1096–1102.
[23] W. Liu, M. Flytzani-Stephanopoulos, J. Catal. 153 (1995) 317.
[24] W.-P. Dow, Y.-P. Wang, T.-J. Huang, Appl. Catal. A: Gen. 190 (2000) 25–34.
[25] U.R. Pillai, S. Deevi, Appl. Catal. B: Environ. 65 (2006) 110–117.
[26] G. Sedmak, S. Hocevar, J. Levec, J. Catal. 213 (2003) 135–150.
[27] J.B. Wang, D.H. Tsai, T.J. Huang, J. Catal. 208 (2002) 370–380.
[28] H. Cordatos, R.J. Gorte, J. Catal. 159 (1996) 112–118.